

504 **A Relation to other self-supervised methods**

505 We compare here VICReg with other methods in terms of methodology, and we discuss the mecha-  
506 nisms used by these methods to avoid collapse and to learn representations, and how they relate to  
507 VICReg. We synthesize and illustrate the differences between these methods in Figure 2.

508 **Relation to Barlow Twins [9].** VICReg uses the same decorrelation mechanism as Barlow Twins,  
509 which consists in penalizing the off-diagonal terms of a covariance matrix computed on the embed-  
510 dings. However, Barlow Twins uses the cross-correlation matrix where each entry in the matrix is a  
511 cross-correlation between two vectors  $z^i$  and  $z^j$ , from the two branches of the siamese architecture.  
512 Instead of using cross-correlations, we simply use the covariance matrix of each branch individually,  
513 and the variance term of VICReg allows us to get rid of standardization. Indeed, Barlow Twins  
514 forces the correlations between pairs of vectors  $z^i$  and  $z^i$  from the same dimension  $i$  to be 1. With-  
515 out normalization, this target value of 1 becomes arbitrary and the vectors take values in a wider  
516 range. Moreover, there is an undesirable phenomenon happening in Barlow Twins, the embeddings  
517 before standardization can shrink and become constant to numerical precision, which could cause  
518 numerical instabilities. In practice, this is solved by adding a constant scalar in the denominator of  
519 standardization of the embeddings. Without normalization, VICReg naturally avoids this edge case.

520 **Relation to W-MSE [16].** The whitening operation of W-MSE consists in computing the inverse  
521 covariance matrix of the embeddings and use its square root as a whitening operator on the embed-  
522 dings. Using this operator has two downsides. First, matrix inversion is a very costly and potentially  
523 unstable operation. VICReg does not need to invert the covariance matrix. Second, as mentioned in  
524 [16] the whitening operator is constructed over several consecutive iteration batches and therefore  
525 might have a high variance, which biases the estimation of the mean-squared error. This issue is  
526 overcome in practice by a batch slicing strategy, where the whitening operator is computed over  
527 randomly constructed sub-batches. VICReg does not apply any operator on the embeddings, but  
528 instead regularizes the variance and covariance of the embeddings using an additional constraint.

529 **Relation to BYOL and SimSiam [6, 7].** The core components that avoid collapse in BYOL and  
530 SimSiam are the average moving weights and the stop-gradient operation on one side of their  
531 asymmetric architecture, which play the role of the repulsive term used in other methods. Our  
532 experiments in Appendix C.5 show that in addition to preventing collapse, these components also  
533 have a decorrelation effect. In addition, we have conducted the following experiment: We compute  
534 the correlation matrix of the final representations obtained with SimSiam, BYOL, VICReg and  
535 VICReg without covariance regularization. We measure the average correlation coefficient and  
536 observe that this coefficient is much smaller for SimSiam, BYOL and VICReg, compared to VICReg  
537 without covariance regularization. We observe in Figure 5 that even without covariance regularization,  
538 SimSiam and BYOL naturally minimize the average correlation coefficient of the representations.  
539 VICReg replaces the moving average weights and the stop-gradient operation, which are architectural  
540 tricks that require some dependency between the branches, by an explicit constraint on the variance  
541 and the covariance of both embeddings separately, which achieves the same goal of decorrelating  
542 the representations and avoiding collapse, while being clearer, more interpretable, and working with  
543 independent branches.

544 **Relation to SimCLR, SwAV and OBoW [5, 12, 8].** Contrastive and clustering based self-supervised  
545 algorithms rely on direct comparisons between elements of negative pairs. In the case of SimCLR, the  
546 negative pairs involve embeddings mined from the current batch, and large batch sizes are required.  
547 Despite the fact that SwAV computes clusters using elements in the current batch, it does not seem  
548 to have the same dependency on batch size. However, it still requires a lot of prototype vectors for  
549 negative comparisons between embeddings and codes. VICReg eliminates the negative comparisons  
550 and replace them by an explicit constraint on the variance of the embeddings, which efficiently plays  
551 the role of a negative term between the vectors. SwAV can also be interpreted as a distillation method,  
552 where a teacher network produces quantized vectors, used as target for a student network. Ensuring  
553 an equal partition of the quantized vectors in different bins or clusters effectively prevents collapse.  
554 OBoW can also be interpreted under the same framework. The embeddings are bag-of-words over a  
555 vocabulary of visual features, and collapse is avoided by the underlying quantization operation.

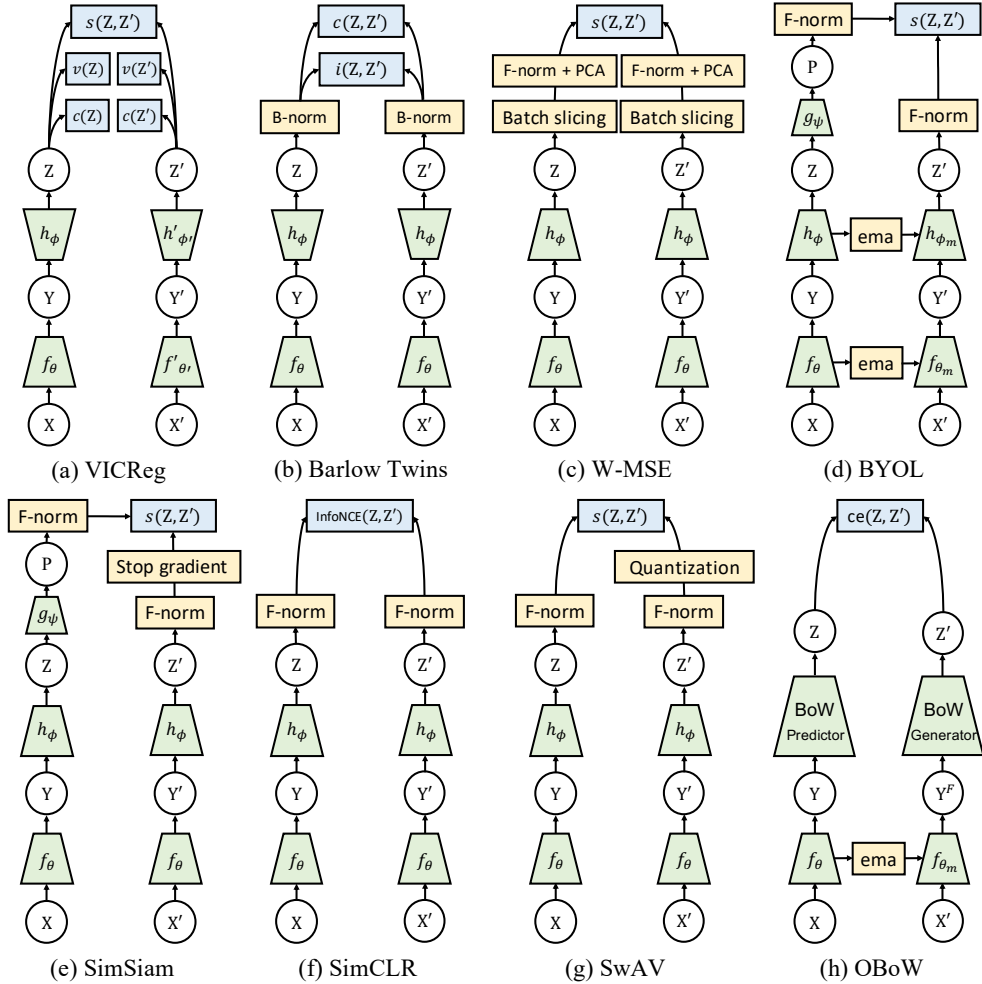


Figure 2: **Conceptual comparison between different self-supervised methods.** The inputs  $X$  and  $X'$  are fed to an encoder  $f$  with weights  $\theta$ . The representations  $Y$  and  $Y'$  are further processed by a network  $h$  with weights  $\psi$ .  $h$  can be a projector (narrowing trapeze) that reduces the dimensionality of the representations, or an expander (widening trapeze) that increases their dimensionality. A criterion is finally applied on the embeddings  $Z$  and  $Z'$ . VICReg (a) works when both branches have encoders  $f$  and  $f'$  with different architectures and sets of weights  $\theta$  and  $\theta'$ . Each branch's variance and covariance are regularized by regularizers  $v$  and  $c$ , and the distance between both branches is minimized with a mean-squared error loss  $s$ . Barlow Twins (b) uses a loss  $c$  to decorrelate pairs of different dimensions in the batch-wise normalized (B-Norm) embeddings, and learns invariance with a loss  $i$  that makes similar dimensions highly correlated. W-MSE (c) uses a batch slicing operation that shuffles batches into small sub-batches, and apply PCA as a whitening operation on the feature-wise normalized (F-Norm) embeddings of each sub-batch. BYOL (d) has an asymmetric architecture where the weights  $\theta_m$  of one encoder are an exponential moving average (ema) of the other encoder's weights  $\theta$ . A predictor  $g$  with weights  $\psi$  is used in the branch with learnable weights. SimSiam (e) uses a predictor on one branch and a stop-gradient operation (sg) on the other one. SimCLR (f) uses the InfoNCE contrastive loss where all the feature-wise normalized embeddings are compared between them inside a batch. Samples from distorted versions of the same input are brought close to each other, while other samples are pushed away. SwAV (g) quantizes the feature-wise normalized embeddings of a branch and use it as target for the other one. OBoW (h) uses bag-of-words (BoW) representations and a cross-entropy loss to compare the BoW generated by a teacher network from the feature maps  $Y^F$  of the encoder, to the BoW predicted by a student network. Green blocks: parametric functions; yellow boxes: non-parametric functions; blue boxes: objective functions.

## 556 B Additional implementation details

### 557 B.1 Data augmentation

558 We follow the image augmentation protocol first introduced in SimCLR [12] and now commonly  
559 used by similar approaches based on siamese networks [5, 6, 7, 9]. Two random crops from the input  
560 image are sampled and resized to  $224 \times 224$ , followed by random horizontal flip, color jittering of  
561 brightness, contrast, saturation and hue, Gaussian blur and random grayscale. Each crop is normalized  
562 in each color channel using the ImageNet mean and standard deviation pixel values. In more details,  
563 the exact set of augmentations is based on BYOL [6] data augmentation pipeline but is symmetrised.  
564 The following operations are performed sequentially to produce each view:

- 565 • Random cropping with an area uniformly sampled with size ratio between 0.08 to 1.0,  
566 followed by resizing to size  $224 \times 224$ . `RandomResizedCrop(224, scale=(0.08,`  
567 `0.1))` in PyTorch.
- 568 • Random horizontal flip with probability 0.5.
- 569 • Color jittering of brightness, contrast, saturation and hue, with probability 0.8.  
570 `ColorJitter(0.4, 0.4, 0.2, 0.1)` in PyTorch.
- 571 • Grayscale with probability 0.2.
- 572 • Gaussian blur with probability 0.5 and kernel size 23.
- 573 • Solarization with probability 0.1.
- 574 • color normalization with mean (0.485, 0.456, 0.406) and standard deviation (0.229, 0.224,  
575 0.225).

### 576 B.2 ImageNet evaluation

577 **Linear evaluation.** We follow standard procedure and train a linear classifier on top of the frozen  
578 representations of a ResNet-50 pretrained with VICReg. We use the SGD optimizer with a learning  
579 rate of 0.02, a weight decay of  $10^{-6}$ , a batch size of 256, and train for 100 epochs. The learning rate  
580 follows a cosine decay. The training data augmentation pipeline is composed of random cropping  
581 and resize of ratio 0.2 to 1.0 with size  $224 \times 224$ , and random horizontal flips. During evaluation the  
582 validation images are simply center cropped and resized to  $224 \times 224$ .

583 **Semi-supervised evaluation.** We train a linear classifier and fine-tune the representations using 1  
584 and 10% of the labels. We use the SGD optimizer with no weight decay and a batch size of 256,  
585 and train for 20 epochs. We perform a grid search on the values of the encoder and linear head  
586 learning rates. In the 10% of labels case, we use a learning rate of 0.01 for the encoder and 0.1 for  
587 the linear head. In the 1% of labels case we use 0.03 for the encoder and 0.08 for the linear head. The  
588 two learning rates follow a cosine decay schedule. The training data and validation augmentation  
589 pipelines are identical to the linear evaluation data augmentation pipelines.

### 590 B.3 Transfer learning

591 We use the VISSL library [48] for linear classification tasks and the detectron2 library [49] for object  
592 detection and segmentation tasks.

593 **Linear classification.** We follow standard protocols [2, 5, 9] and train linear models on top of the  
594 frozen representations. For VOC07 [43], we train a linear SVM with LIBLINEAR [50]. The images  
595 are center cropped and resized to  $224 \times 224$ , and the C values are computed with cross-validation.  
596 For Places205 [42] we use SGD with a learning rate of 0.003, a weight decay of 0.0001, a momentum  
597 of 0.9 and a batch size of 256, for 28 epochs. The learning rate is divided by 10 at epochs 4, 8 and  
598 12. For Inaturalist2018 [44], we use SGD with a learning rate of 0.005, a weight decay of 0.0001, a  
599 momentum of 0.9 and a batch size of 256, for 84 epochs. The learning rate is divided by 10 at epochs  
600 24, 48 and 72.

601 **Object detection and instance segmentation.** Following the setup of [3, 9], we use the `trainval`  
602 split of VOC07+12 with 16K images for training and a Faster R-CNN C-4 backbone for 24K iterations  
603 with a batch size of 16. The backbone is initialized with our pretrained ResNet-50 backbone. We  
604 use a learning rate of 0.1, divided by 10 at iteration 18K and 22K, a linear warmup with slope of  
605 0.333 for 1000 iterations, and a region proposal network loss weight of 0.2. For COCO we use Mask  
606 R-CNN FPN backbone for 90K iterations with a batch size of 16, a learning rate of 0.04, divided by  
607 10 at iteration 60K and 80K and with 50 warmup iterations.

## 608 B.4 Ablation studies

609 We give here implementation details on the results of Table 3 with BYOL and SimSiam, as well as the  
610 default setup for VICReg with 100 epochs of pretraining, used in all our ablations. For both BYOL  
611 and SimSiam experiments, the variance criterion has coefficient  $\mu = 1$  and the covariance criterion  
612 has coefficient  $\nu = 0.01$ , the data augmentation pipeline and the architectures of the expander and  
613 predictor exactly follow the pipeline and architectures described in their paper. The linear evaluation  
614 setup of each methods follows closely the setup described in the original papers.

615 **BYOL setup.** We use our own BYOL implementation in PyTorch, which outperforms the original  
616 implementation for 100 epochs of pretraining (69.3% accuracy on the linear evaluation protocol  
617 against 66.5% for the original implementation) and matches its performance for 1000 epochs of  
618 pretraining. We use the LARS optimizer [37], with a learning rate of  $base\_lr * batch\_size / 256$   
619 where  $base\_lr = 0.45$ , and  $batch\_size = 4096$ , a weight decay of  $10^{-6}$ , an eta value of 0.001 and  
620 a momentum of 0.9, for 100 epoch of pretraining with 10 epochs of warmup. The learning rate  
621 follows a cosine decay schedule. The initial value of the exponential moving average factor is 0.99  
622 and follows a cosine decay schedule.

623 **SimSiam setup.** We use our own implementation of SimSiam, which reproduces exactly the per-  
624 formance reported in the paper [7]. We use SGD with a learning rate of  $base\_lr * batch\_size / 256$   
625 where  $base\_lr = 0.05$ ,  $batch\_size = 2048$ , with a weight decay of 0.0001 and a momentum of 0.9  
626 for 100 epochs of pretraining and 10 epochs of warmup. The learning rate of the encoder and the  
627 expander follow a cosine decay schedule while the learning rate of the predictor is kept fixed.

628 **VICReg setup.** The setting of VICReg’s experiments is identical to the setting described in sec-  
629 tion 4.2, except that the number of pretraining epochs is 100 and the base learning rate is 0.3. The  
630 base learning rates used for the batch size study are 0.8, 0.5 and 0.4 for batch size 128, 256 and 512  
631 respectively, and 0.3 for all other batch sizes. When a predictor is used, it has a similar architecture  
632 as the expander described in section 4.2, but with 2 layers instead of 3, which gives better results in  
633 practice.

## 634 C Additional results

### 635 C.1 Other ResNet architectures

636 Table 7 reports the performance of VICReg on linear classification with large ResNet architectures.  
637 We focus on the wider family of ResNet [51] and aggregated ResNet [52], and we consider two ways  
638 of widening a standard ResNet. First, we follow standard practice in recent self-supervised learning  
639 work [5, 6, 12] and multiple by 2 or 4 the number of filters in every convolutional layer, which also  
640 has the effect of multiplying the dimensionality of the representations. Second, as originally proposed  
641 in [51], we only multiply the number of filters in the bottleneck layers, which does not increase the  
642 dimensionality of the representations. We call this architecture Narrow ResNet (with prefix N- in  
643 Table 7). The main observation we make is the dependency of VICReg on the dimensionality of the  
644 representation. Using the narrow architecture, the performance of VICReg, jumps from 73.2% top-1  
645 accuracy on linear classification with a ResNet-50, to 74.7% with Narrow ResNet-50 (x2), which is  
646 a 1.5% improvement and 76.0% with Narrow ResNet-50 (x4), which is a 2.8% improvement. We  
647 observe a similar trend going from ResNet-50 to ResNet-50 (x2), which is a 2.3% improvement  
648 but the performance completely saturates with ResNet-50 (x4), which is a 0.1% improvement over  
649 ResNet-50 (x2). Table 8 reports the performance of VICReg on semi-supervised classification with  
650 large ResNet architectures. VICReg combined with a ResNet-50 (x2) outperforms the current  
651 state-of-the-art methods BYOL and SimCLR, using this encoder architecture. Our largest model  
652 ResNet-200 (x2) performs lower than BYOL when 1% of the labels are used but is on par with 10% of  
653 the labels. These results demonstrate the capabilities of VICReg to scale up when large architectures  
654 are used.

### 655 C.2 K-nearest-neighbors

656 Following recent protocols [5, 21, 28], we evaluate the learnt representations using K-nearest-  
657 neighbors classifiers built on the training set of ImageNet and evaluated on the validation set of  
658 ImageNet. We report the results with K=20 and K=200 in Table 9. VICReg performs slightly lower  
659 than other methods in the 20-NN case but remains competitive in the 200-NN case. These results  
660 with K-NN classifiers demonstrate the potential applicability of VICReg to downstream tasks based  
661 on nearest neighbors search, such as content retrieval in images or videos.

Table 7: **Linear classification with large architectures.** Top-1 accuracy comparison between different methods using various encoder architectures. For all VICReg results, the output dimensionality of the expander is 8192. N-R stands for Narrow ResNet, where only the bottleneck convolutional layers are widen.

Method	Arch.	Param.	Repr.	Top-1	Top-5
SimCLR [12]	R50 (x2)	93M	4096	74.2	92.0
	R50 (x4)	375M	8192	76.5	93.2
SwAV [5]	R50 (x2)	93M	4096	77.3	-
	R50 (x4)	375M	8192	77.9	-
	R50 (x5)	586M	10240	78.5	-
BYOL [6]	R50 (x2)	93M	4096	77.4	93.6
	R50 (x4)	375M	8192	78.6	94.2
	R200 (x2)	250M	4096	79.6	94.8
VICReg (ours)	N-R50 (x2)	66M	2048	74.7	91.9
	N-R50 (x4)	221M	2048	76.0	92.4
	R50 (x2)	93M	4096	75.5	92.1
	R50 (x4)	375M	8192	75.6	92.2
	RNXT101-32-16	191M	2048	76.1	92.3
	R200 (x2)	250M	4096	77.3	93.3

Table 8: **Semi-supervised classification with large architectures.** Top-1 accuracy comparison between different methods using various encoder architectures. For all VICReg results, the output dimensionality of the expander is 8192.

Method	Arch.	Param.	Repr.	Top-1		Top-5	
				1%	10%	1%	10%
SimCLR [12]	R50 (x2)	93M	4096	58.5	71.7	83.0	91.2
	R50 (x4)	375M	8192	63.0	74.4	85.8	92.6
BYOL [6]	R50 (x2)	93M	4096	62.2	73.5	84.1	91.7
	R50 (x4)	375M	8192	69.1	75.7	87.9	92.5
	R200 (x2)	250M	4096	71.2	77.7	89.5	93.7
VICReg (ours)	R50 (x2)	93M	4096	62.6	73.9	84.5	91.8
	R200 (x2)	250M	4096	68.8	77.3	88.2	93.6

Table 9: **K-NN classifiers on ImageNet.** Top-1 accuracy with 20 and 200 nearest neighbors.

Method	20-NN	200-NN
NPID [21]	-	46.5
LA [28]	-	49.4
PCL [53]	54.5	-
BYOL [6]	66.7	64.9
SwAV [5]	65.7	62.7
Barlow Twins [9]	64.8	62.9
VICReg	64.5	62.8

Table 10: **Impact of expander dimensionality.** Top-1 accuracy on the linear evaluation protocol with 100 pretraining epochs.

Dimensionality	256	512	1024	2048	4096	8192	16834
Top-1	55.9	59.2	62.4	65.1	67.3	68.6	68.8

Table 11: **Impact of batch size.** Top-1 accuracy on the linear evaluation protocol with 100 pretraining epochs.

Batch size	128	256	512	1024	2048	4096
Top-1	67.3	67.9	68.2	68.3	68.6	67.8

### 662 C.3 Expander network architecture

663 VICReg borrows the decorrelation mechanism of Barlow Twins [9] and we observe that it therefore  
 664 has the same dependency on the dimensionality of the expander network. Table 10 reports the impact  
 665 of the width and depth of the expander network. The dimensionality corresponds the number of  
 666 hidden and output units in the expander network during pretraining. As the dimensionality increases,  
 667 the performance dramatically increases from 55.9% top-1 accuracy on linear evaluation with a  
 668 dimensionality of 256, to 68.8% with dimensionality 16384. The performance tends to saturate as the  
 669 difference between dimensionality 8192 and 16384 is only of 0.2%.

### 670 C.4 Batch size

671 Contrastive methods suffer from the need of a lot of negative examples which can translate into the  
 672 need for very large batch sizes [12]. Table 11 reports the performance on linear classification when  
 673 the size of the batch varies between 128 and 4096. For each value of batch size, we perform a grid  
 674 search on the base learning rate described in Appendix B.4. We observe a 0.7% and 1.2% drop in  
 675 accuracy with small batch size of 256 and 128 which is comparable with the robustness to batch  
 676 size of Barlow Twins [9] and SimSiam [7], and a 0.8% drop with a batch size of 4096, which is  
 677 reasonable and allows our method to be very easily parallelized on multiple GPUs.

### 678 C.5 Combination with BYOL and SimSiam

679 BYOL [6] and SimSiam [7] rely on a effective but difficult to interpret mechanism for preventing  
 680 collapse, which may lead to instabilities during the training. We incorporate our variance regular-  
 681 ization loss into BYOL and SimSiam and show that it helps stabilize the training and offers a small  
 682 performance improvement. For both methods, the results are obtained using our own implementation  
 683 and the exact same data augmentation and optimization settings as in their original paper. The  
 684 variance and covariance regularization losses are incorporated with a factor of  $\mu = 1$  for variance and  
 685  $\nu = 0.01$  for covariance. We report in Figure 3 the improvement obtained over these methods on the  
 686 linear evaluation protocol for different number of pre-training epochs. For BYOL the improvement is  
 687 of 0.9% with 100 epochs and becomes less significant as the number of pre-training epochs increases  
 688 with a 0.2% improvement with 1000 epochs. This indicates that variance regularization makes BYOL  
 689 converge faster. In SimSiam the improvement is not as significant. We plot in Figure 4 the evolution  
 690 of the standard deviation computed along each dimension and averaged across the dimensions of the  
 691 representation and the embeddings, during BYOL and SimSiam pretraining. For both methods, the  
 692 standard deviation computed on the embeddings perfectly matches  $1/\sqrt{d}$  where  $d$  is the dimension  
 693 of the embeddings, which indicates that the embeddings are perfectly spread-out across the unit  
 694 sphere. This translates in an increased standard deviation at the representation level, which seems  
 695 to be correlated to the performance improvement. We finally study in Figure 5 the evolution of the  
 696 average correlation coefficient, during pretraining of BYOL and SimSiam, with and without variance  
 697 and covariance regularization. The average correlation coefficient is computed by averaging the  
 698 off-diagonal coefficients of the correlation matrix of the representations:

$$\frac{1}{2d(d-1)} \sum_{i \neq j} C(Y)_{i,j}^2 + C(Y')_{i,j}^2, \quad (9)$$

699 where  $Y$  and  $Y'$  are the standardized representations and  $C$  is defined in Eq. (3). In BYOL this  
 700 coefficient is much lower using covariance regularization, which translate in a small improvement of

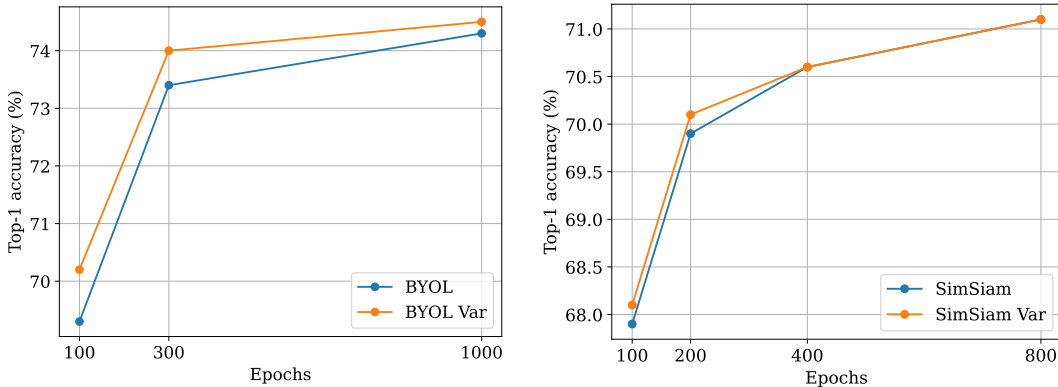


Figure 3: **Incorporating variance regularization in BYOL and SimSiam.** Top-1 accuracy on the linear evaluation protocol for different number of pretraining epochs. For both methods pre-training follows the optimization and data augmentation protocol of their original paper but is based on our implementation. *Var* indicates variance regularization

701 the performance, according to Table 3. We do not observe the same improvement in SimSiam, both  
 702 in terms of correlation coefficient, and in terms of performance on linear classification. The average  
 703 correlation coefficient is correlated with the performance, which motivates the fact that decorrelation  
 704 and redundancy reduction are core mechanisms for learning self-supervised representations.

#### 705 D Running time

706 We report in Table 12, the running time of VICReg in comparison with other methods. All methods  
 707 are run by us on 32 Tesla V100 GPUs. Each method offers a different trade-off between running  
 708 time, memory and performance. SwAV is a very fast algorithm which use less memory and run faster  
 709 than the other methods but with a lower performance, multi-crop helps the performance at the cost of  
 710 additional compute and memory usage. BYOL has the highest memory requirement, which is due to  
 711 the need of storing the target network weights. Finally, Barlow Twins and VICReg offer an interesting  
 712 trade-off, consuming less memory than BYOL and SwAV with multi-crop, and running faster than  
 713 SwAV with multi-crop, but with a slightly worse performance. The difference of 1h running time  
 714 between Barlow Twins and VICReg is probably due to implementation details not related to the  
 715 method.

Table 12: **Running time and peak memory.** Comparison between different methods, the training is distributed on 32 Tesla V100 GPUs, the running time is measured over 100 epochs and the peak memory is measured on a single GPU. We report top-1 accuracy (%) on linear classification on top of the frozen representations.

Method	time / 100 epochs	peak memory / GPU	Top-1 accuracy (%)
SwAV	9h	9.5G	71.8
SwAV (w/ multi-crop)	13h	12.9G	75.3
BYOL	10h	14.6G	74.3
Barlow Twins	12h	11.3G	73.2
VICReg	11h	11.3G	73.2

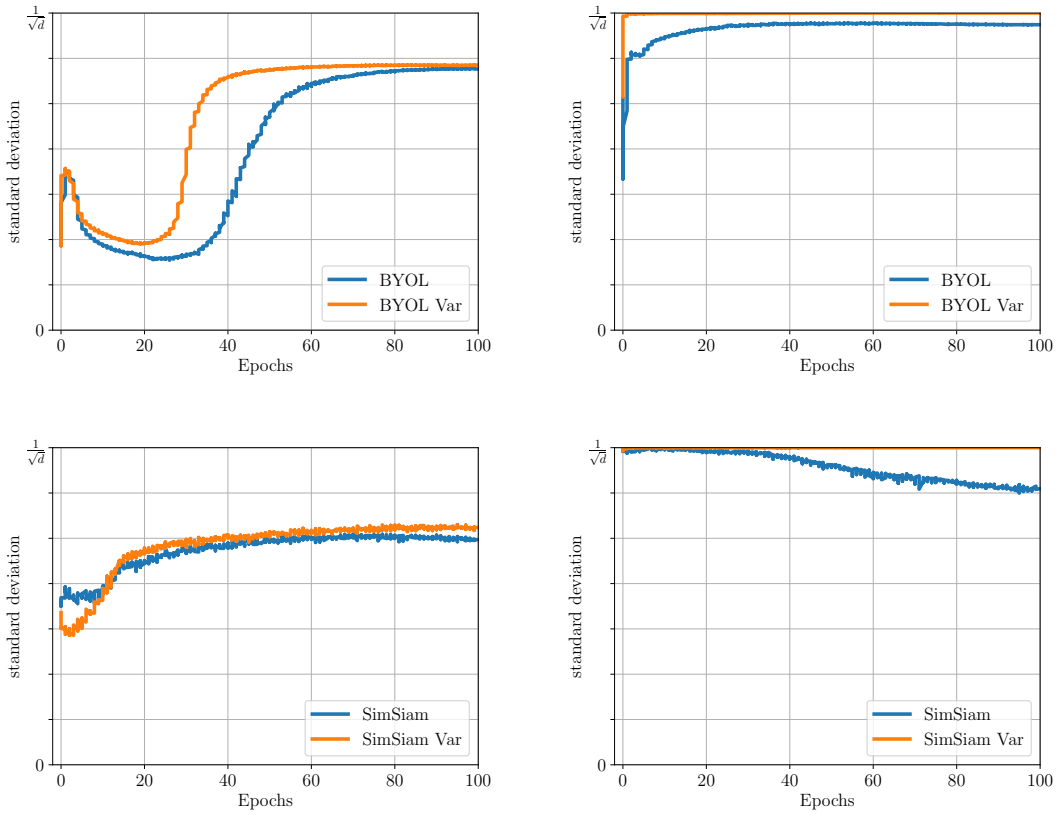


Figure 4: **Standard deviation of the features during BYOL and SimSiam pretraining.** Evolution of the average standard deviation of each dimension of the features with and without variance regularization (Var). left: the standard deviation is measured on the representations, right: the standard deviation is measured on the embeddings.

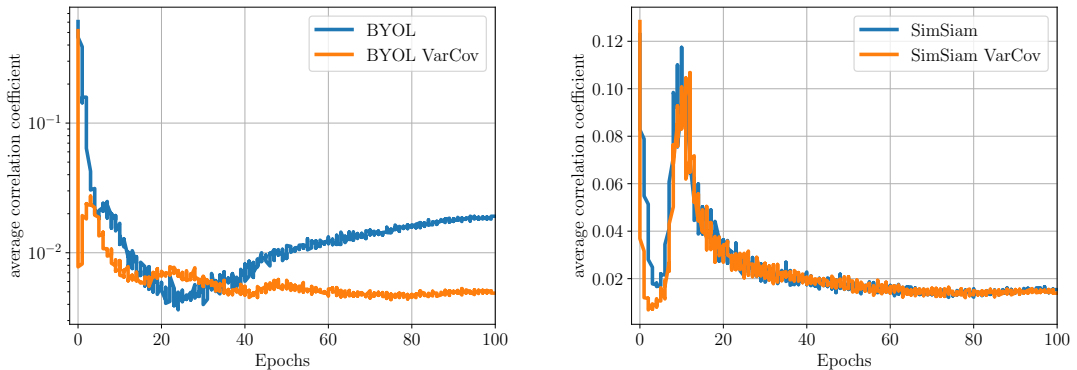


Figure 5: **Average correlation coefficient of the features during BYOL and SimSiam pretraining.** Evolution of the average correlation coefficient measured by averaging the off-diagonal terms of the correlation matrix of the representations with BYOL, BYOL with variance-covariance regularization (BYOL VarCov), SimSiam, and SimSiam with variance-covariance regularization (SimSiam VarCov).